Computing Fermi Contact Shifts using CRYSTAL

Euan N. Bassey

June 8, 2024

1 Setting the scene

This document is designed to act as a guide to computing the Fermi contact shift using CRYSTAL. It assumes the user is familiar (but not an expert) in python, bash, and has access to the CRYSTAL executables on a cluster. We will begin by briefly introducing the hyperfine interaction in paramagnetic solids and its influence on a solid-state nuclear magnetic resonance (NMR) spectrum. From here, we will discuss how to compute the Fermi contact shifts using CRYSTAL in three steps: (1) a spin-locked calculation; (2) a spin-relaxed calculation; and (3) properties extraction. From the properties, we describe how to use a python script to determine the shifts at experimentally relevant fields and temperatures.

2 The Hyperfine Interaction

In the presence of a magnetic field, both the nuclear and electronic spin states of a paramagnetic material are split *via* the *Zeeman interaction*.[i] Compared to the NMR timescale, the relaxation of electronic microstates is rapid. Therefore, the nuclear magnetic moments in the sample interact with the time-averaged magnetic moment of the electron spins, $\langle \mu_e \rangle$, rather than with individual electronic spin microstates. This interaction is known as hyperfine coupling and can result in significantly larger

[i] The Zeeman interaction describes the interaction between a spin, $\mathbf{S}$, and a magnetic field, $\mathbf{B}$. Note that the symbol $\mathbf{B}$ is strictly reserved for the magnetic flux density, related to the applied magnetic field strength, $\mathbf{H}$, by $\mathbf{B} = \mu_0(\mathbf{M} + \mathbf{H})$. Throughout this tutorial, we will assume the magnetic susceptibility, $\boldsymbol{\chi} = \mathbf{M}/\mathbf{H}$, is much less than one, so the applied field strength and flux density are, to all intents and purposes, equal.

shifts than those observed in diamagnetic spectra. The Hamiltonian for the hyperfine coupling is:

$$\hat{\mathcal{H}}_{\text{hf}} = \hat{\mathbf{S}} \cdot \mathbf{A} \cdot \hat{\mathbf{I}}, \tag{1}$$

where $\hat{\mathbf{S}}$ and $\hat{\mathbf{I}}$ are the electronic and nuclear spin operators, respectively, and $\mathbf{A}$ the hyperfine interaction tensor. It turns out that[ii] $\mathbf{A}$ may be divided into an isotropic *Fermi contact* coupling term and a traceless, symmetric *spin-dipolar* tensor, $\mathbf{A}^{\text{SD}}$:

$$\mathbf{A} = A^{\text{FC}}\mathbf{1} + \mathbf{A}^{\text{SD}}, \tag{2}$$

where $\mathbf{1}$ is the 3×3 identity matrix. In solids, we typically expect the electrons to occupy crystalline orbitals, delocalised over all centres in the crystal. Consequently, there is a finite probability that an unpaired electron originating from a paramagnetic centre (*e.g.*, a transition metal, *TM*) will delocalise onto nearby diamagnetic species (*e.g.*, a ligand): this is known as the *delocalisation mechanism*. Furthermore, unpaired electrons primarily localised to one paramagnetic centre may, in addition to delocalising, spin-polarise nearby diamagnetic electrons (*via* Hund's rules): this is known as the *polarisation mechanism*. Both mechanisms are responsible for generating a finite amount of unpaired electron spin density at or nearby a nucleus, resulting in a hyperfine interaction. The Fermi contact interaction is generally responsible for the large-magnitude isotropic shifts seen in paramagnetic materials, whilst the spin dipolar interaction dominates the spinning sideband manifold.

2.1 The Fermi Contact Interaction

The Fermi contact interaction is an orbital-mediated process, where unpaired electron spin density is transferred from a paramagnetic centre to the nucleus of interest, X.[iii] One can write the isotropic Fermi contact coupling as:

$$A^{\text{FC}} = \frac{\mu_0 \mu_{\text{B}} \mu_{\text{N}} g_{\text{e}} g_{\text{N}} |\psi^{\alpha-\beta}(\mathbf{R}_{\text{N}})|^2}{3S}, \tag{3}$$

[ii] A cure-all phrase which here means that there is no intention of deriving this here, but rest assured the result is true.

[iii] The Fermi contact interaction can only occur *via* spin density transfer (delocalisation- or polarisation-driven) from a paramagnetic centre to the s orbitals on X, since these are the only orbitals which have non-zero electron density at the nuclear position.

where μ_0 is the permittivity of free space; μ_B the Bohr magneton; μ_N the nuclear magneton; g_e and g_N the free-electron and nuclear g-factors, respectively; $|\psi^{\alpha-\beta}(\mathbf{R}_N)|^2$ is the unpaired spin density at the nuclear position and S is the total electronic spin. The Fermi contact hyperfine coupling results in a shift, δ^{FC}, which invariably overwhelms the isotropic shift observed in an NMR spectrum:

$$\delta^{FC} = \frac{2SA^{FC}\chi_M}{N_A\mu_0\mu_B\mu_N g_e g_N}, \tag{4}$$

where χ_M is the molar magnetic susceptibility and N_A is Avogadro's number. As δ^{FC} depends on the magnetic susceptibility, it is possible to extract information about the paramagnetic behaviour of a material from its paramagnetic shift. The extent of spin transfer—and therefore the value of δ^{FC}—depends on the degree of orbital overlap along the pathway between the paramagnetic centre and X: this is termed the *bond pathway* and, as we shall see, can allow us to readily predict hyperfine shifts of highly disordered materials without having to re-compute the shift in all possible local environments.

The relative magnitudes and signs of the spin density transferred along a bond pathway may be qualitatively rationalised using the Gooednough-Kanamori-Anderson rules. As a concrete example, let us imagine two scenarios: firstly, a lithium ion which is bonded to a transition metal (*TM*) centre *via* an intermediary O^{2-} ligand with a bond angle of 90°; secondly, the same Li^+–O^{2-}–*TM* configuration, now with a 180° angle. Both are depicted in Figure 1 in terms of the relative energies of different local molecular orbitals of the Li^+–O^{2-}–*TM* unit. We recall that the *s* orbitals are those which will generate electron spin density at the nuclear position ($|\psi^{\alpha-\beta}(\mathbf{R}_N)|^2$ in eq. 3) which, in the case of Li^+, are vacant. In the case of *TM* oxides, the highest-energy orbitals are usually either non-bonding or (weakly) anti-bonding in nature. Recall also that the *d*-orbitals on the *TM* cations which point between bonds typically have t_{2g} symmetry and overlap side-on with ligand orbitals ("π-like"), while those *d* orbitals along bonds typically have e_g symmetry and overlap head-on ("σ-like").

For a 90° pathway, one can envisage four scenarios of overlap: two of π-like character and two σ-like. There are two of each type because the bond pathway could derive from a high-energy, fully-occupied, spin-polarised orbital, or from a partially occupied frontier orbital. Vacant orbitals

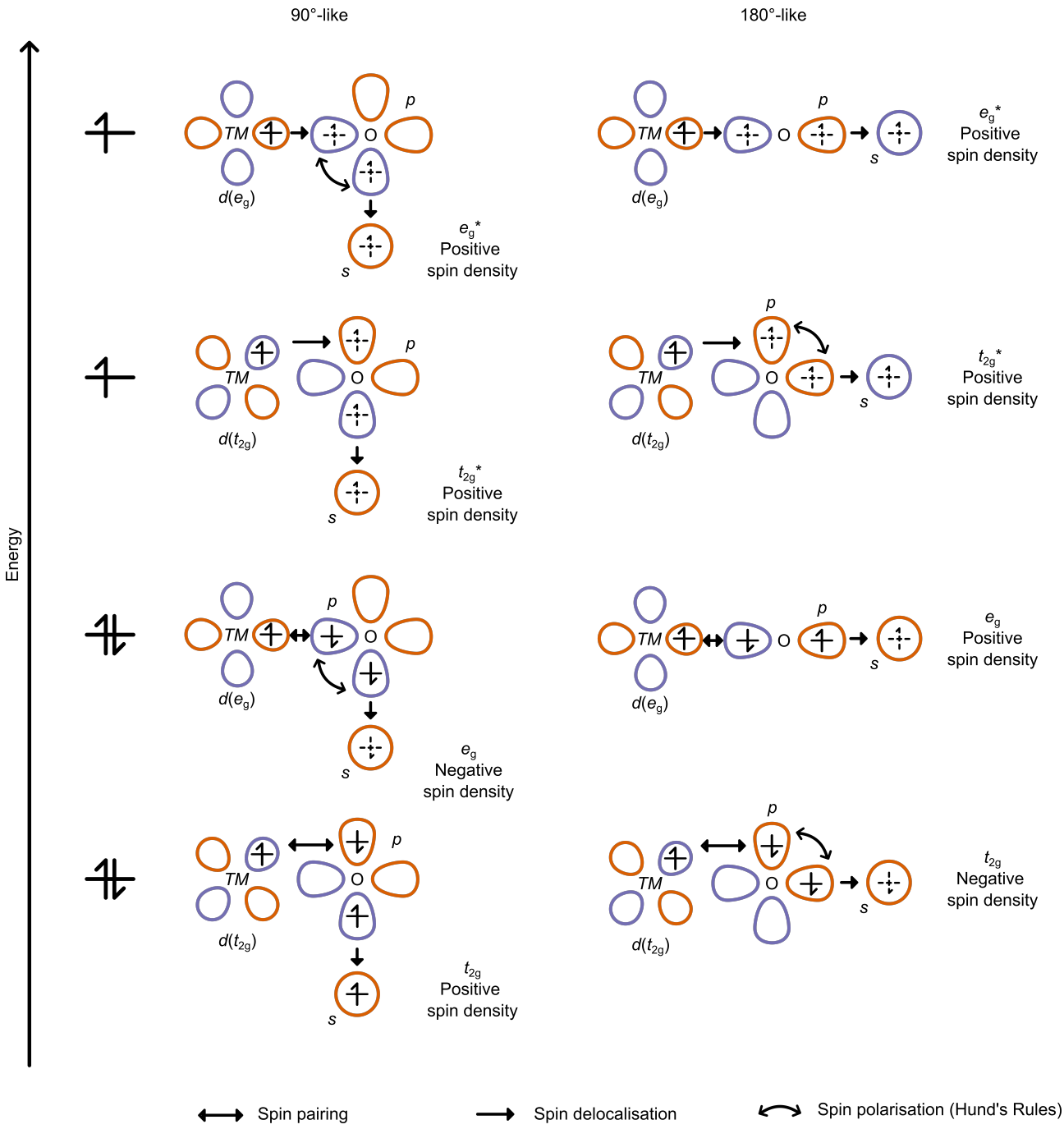

Figure 1: Illustrations showing the Fermi-contact hyperfine interaction for two representative *TM* to Li pathways in Li_xTMO_2 materials. The polarised spins are denoted using dashed spins. The bottom two schematics illustrate spin delocalisation; the top two illustrate spin polarisation (and delocalisation).

are unlikely to contribute to the shift, as these do not contain any electron density. For the sake of simplicity, we shall focus on the bond pathway from the perspective of the O^{2-} [Figure 1, bottom left]. If we were to imagine that the O^{2-} is the source of electrons in this orbital, then the electrons which sit, on average, closer to the *TM* cation in the *TM*–O^{2-} bond will be spin-polarised by the unpaired electrons on the *TM*; conventionally, this is assumed to be "up".[iv] Correspondingly, those electrons which, on average, sit closer to O^{2-} must be polarised mostly down in order to ensure electrons in the *TM*–O^{2-} bond are spin-paired, as per Hund's rules. Since the O^{2-} has filled *p* orbitals, then to ensure Hund's rules are obeyed on O^{2-}, the electron sitting in the *p* lobe closer to Li^+ must be mostly spin up. As the Li^+ *s* orbital is vacant, the O^{2-} electron will delocalise onto the Li^+ *s* orbital, giving net positive spin density on Li^+ *s*. It is important to note that, in this "virtual electron hopping" scheme we have just derived, only two electrons are delocalised across the Li^+–O^{2-}–*TM* unit: we can break this down into the two constituent bonds within this unit to work out how the up and down electrons are distributed. In the case of a part-filled π-like interaction, only one electron can delocalise and so the Li^+ *s* orbital acquires the same sign of polarisation as the *TM* [Figure 1, second from top, left]. Both of these pathways rely solely on the *delocalisation* mechanism of spin transfer.

For a σ-like interaction along a 90° pathway, there are two orbitals involved along the bond pathway: one along the *TM*–O^{2-} bond, and one along the O^{2-}–Li^+ bond; these bonds are, by construction, perpendicular [Figure 1, second from bottom, left]. Along the *TM*–O^{2-} bond, one can (again) assign electrons which sit closer to the *TM* as having more "up" character, with those sitting closer to O^{2-} correspondingly having more "down" character. Hund's rules dictate that electrons in different orbitals on the same species will prefer to align parallel than anti-parallel (known as a *polarisation* mechanism of spin transfer); as such, the electrons on the O^{2-} *p* involved in the O^{2-}–Li^+ bond will also have more "down" character. The "down"-like electrons on O^{2-} will delocalise onto the vacant Li^+ *s* orbital to give a negative spin density at the nuclear position. A half-filled σ-like orbital will, as in the π-like case, result in the same sign polarisation on Li^+ *s* as the *TM* [Figure 1, top left].

Now turning to the 180° pathway: in the case of a filled π-like interaction, two orthogonal orbitals

[iv] This is not *entirely* arbitrary. When placed in a strong magnetic field (such as the fields at which NMR experiments are performed), the unpaired electrons on the *TM* cations will tend to align with the field, as this is the lower-energy microstate (in the absence of strong magnetic exchange couplings).

are involved, as in the 90° σ-like interaction [Figure 1, bottom right]. For the *TM*–O^{2-} bond, electrons closer to the *TM* will, on average, be polarised spin "up" and as such those nearer the O^{2-} are mostly spin "down". Invoking Hund's rules for exchange between orthogonal *p* orbitals on O^{2-} gives a net "down" spin on the O^{2-} *p* orbital pointing towards Li^+, so the Li^+ *s* acquires overall "down" spin by delocalisation. Part-filling this orbital again leads to the same sign polarisation on Li^+ *s* as the *TM* [Figure 1, second from top, right].

Finally, for the filled σ-like 180° pathway, only one orbital is involved, analogous to the 90° π path. Focusing initially on the *TM*–O^{2-} bond only, electrons which are closer to the *TM* will have more "up" character, while those nearer O^{2-} will be more "down" like. As the O^{2-} *p* orbital is full, the lobe pointing towards the vacant Li^+ *s* orbital must be mostly "up" character; this delocalises onto the *s*, giving overall "up" character to the Li^+ *s* orbital. Making the σ-like 180° orbital part-filled yields direct transfer of electron density from the *TM* to Li^+ with the same sign polarisation [Figure 1, top right].

Clearly, almost all bond pathways will involve some admixture of the 90° and 180° interactions, as no pathway will be exactly at 90° or 180°. One must think carefully, therefore, about the degree to which the 90° and 180° will dominate (based on the overall angle and symmetry of the interaction) and, within each of these angles, whether filled or part-filled σ- or π-like interactions will dominate. In general, we can construct qualitative rules to guide our intuition about the relative signs and sizes of bond pathways:

- If the symmetries of the *TM* and ligand orbitals are the same, their orbitals must overlap and spin delocalisation will dominate.
- If the symmetries of the *TM* and ligand orbitals differ, these orbitals may not mix, and polarisation will instead dominate.
- In general, delocalisation is stronger than polarisation, as it requires fewer orbitals to transfer spin density from one centre to another.
- In general, σ-like interactions will be stronger than π-like.

2.2 Overview of the Computational Approach

Based on the above arguments, one can begin to construct a qualitative picture of the signs and sizes of bond pathways between a *TM* and its nearby ligands; exact evaluation, however, is not feasible and typically requires quantum-chemical calculations. Computing these shifts can be done in CRYSTAL: the wavefunction for the system is determined assuming a (often fictitious) ferromagnetic ground state—*i.e.*, the electron spins on all paramagnetic centres are fixed to be parallel. Whilst this magnetic state is not (in general) a true description of the $T = 0$ K magnetic structure of the material, this state is more convenient in density functional theory (DFT) calculations. To ensure good convergence of this state and ensure the spin densities are determined accurately, the calculations proceed via the following steps:

1. Perform a geometry optimisation using 'contracted' basis sets (i.e., bases which contain the bare minimum number of functions required to describe the orbitals) when the spins of all TM ions are fixed parallel to each other (a 'spin-locked' state);

2. Re-optimise the structure from step (1), this time starting from the 'spin-locked' converged wavefunctions, without any spin constraints in place;

3. Using the optimised structure, begin a single-point energy calculation using a set of 'extended' basis sets (i.e., bases which describe the electronic structure of the ions accurately, by including unoccupied valence orbitals in its description) with all TM spins fixed parallel to each other;

4. Run a final single-point energy calculation on the converged wavefunction from step (3), this time removing the constraints on the relative spin orientations.

Using the converged wavefunction from step (4) above, the spin densities, $|\psi^{\alpha-\beta}(\mathbf{R}_\mathrm{N})|^2$, may be extracted and converted into shifts. Note that steps (1) and (2) need not be done in CRYSTAL: one can start with a pre-relaxed structure from other DFT codes, or even from a crystal structure obtained experimentally. Be aware that CRYSTAL can struggle with configurations (structures) which are very high in energy!

2.3 Bond pathways

When there are several paramagnetic species present (for example, Ni^{2+}, Co^{4+} and Mn^{4+}, as seen in paramagnetic Li-ion battery cathode materials), one can break down the overall shift of a Li-ion into its constituent bond pathways, δ_j^{path}, assuming that these bond pathways are non-interacting:[v]

$$\delta_i^{\text{FC}} = \sum_{\langle i,j \rangle} z_j \delta_j^{\text{path}}. \tag{5}$$

Here, the summation is conventionally taken over the nearest and next-nearest neighbour coordination shell, j, around a central atom, i; the multiplicity of the pathways are given by z_j. It is recommended that one evaluates the sizes of bond pathways of more distant coordination shells to see whether additional (or even fewer) terms are required. The evaluation of δ_j^{path} is conventionally done using "spin-flip" calculations of the Fermi contact shift, where the a single paramagnetic spin is flipped from "up" to "down". In doing so, one can evaluate a pathway *via*:

$$\delta_j^{\text{path}} = \frac{\delta_i^{\text{FC, ferro}} - \delta_i^{\text{FC, flip } j}}{2}, \tag{6}$$

where $\delta_i^{\text{FC, ferro}}$ is the Fermi contact shift for site i computed in a ferromagnetic cell and $\delta_i^{\text{FC, flip } j}$ the Fermi contact shift for site i computed after flipping the j^{th} spin in the nearest or next-nearest coordination shell of site i.

3 Computing the Fermi Contact Shift

3.1 Step 0: The Structure

Having covered the basics of Fermi contact shifts, we are now in a position to begin calculating. We will begin by looking at a crystal structure and establishing an appropriate size and shape for a calculation. Throughout this tutorial we will use a layered Li-ion cathode, Li_2MnO_3, as an example.

[v] This is not always the case: the bond pathways may—and indeed often do—interact, for example in the presence of residual magnetic exchange couplings between paramagnetic centres, or strongly anisotropic local coordination environments, where increased orbital mixing is promoted.

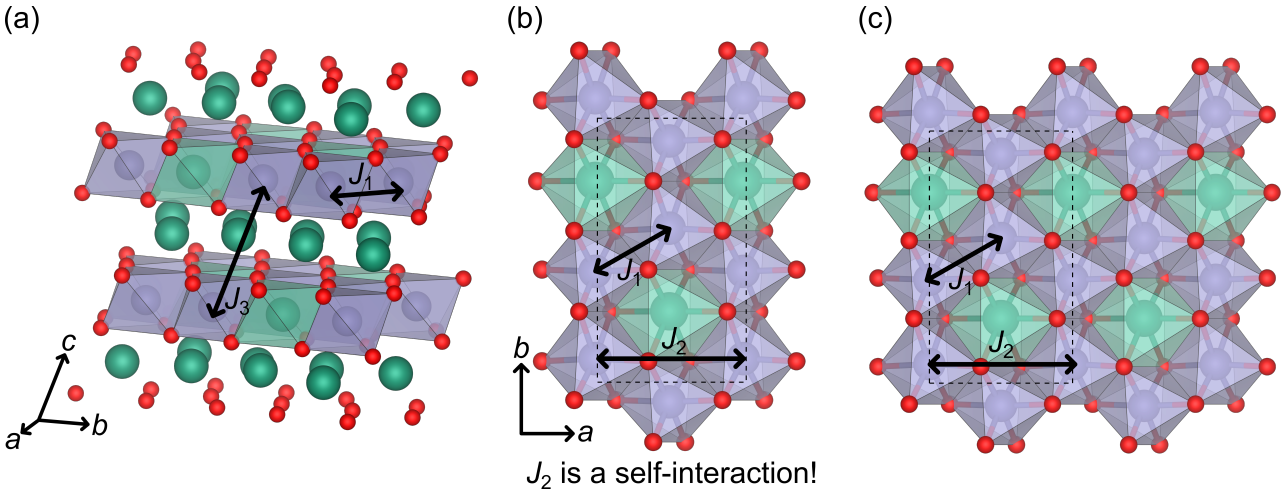

Figure 2: Structure of Li_2MnO_3. In **(a)**, the crystallographic unit cell is shown, alongside the interlayer nearest neighbour, J_1, and next-next-nearest neighbour, J_3, magnetic exchange pathways highlighted. In **(b)**, the view down the c-axis is shown, with J_1 and the next-nearest neighbour, J_2, magnetic exchange pathways shown. In this cell, J_2 is a self-interaction. Therefore, a $(2 \times 1 \times 1)$ supercell, shown in **(c)**, is required to accurately describe the nearest, next-nearest and next-next-nearest exchange interactions.

1. Open your crystal structure in a structure visualization software (here, VESTA, but other applications such as CrystalMaker or Ovito will also suffice)

2. Remove all symmetry from the unit cell if not done already

3. Ask yourself: what are the possible magnetic exchange interaction pathways present in your material? Up to what distance do you expect these couplings to be observed? Commonly in inorganic systems with atomic linkers between paramagnetic centres, only up to the third nearest-neighbour is required. *e.g.*, in Li_2MnO_3, we need a cell which contains the three nearest-neighbour exchange pathways (J_1, J_2 and J_3 in Figure 2). Whilst a $(1 \times 1 \times 1)$ cell will capture J_1 and J_3 accurately [Figure 2(a)], it captures J_2 as a self-interaction. Accordingly, we must build a $(2 \times 1 \times 1)$ supercell [Figure 2(c)] to avoid this self-interaction error.

4. Having built an appropriate size supercell, we now must export our structure as a POSCAR (VASP) format - this can be done in all the above listed crystallographic software packages.

The reason capturing these exchange interactions is important is that these interactions directly

impact the spin transfer pathways: if we can successfully model exchange and capture these interactions, we have a better chance of accurately computing the Fermi contact shift.

3.2 Step 1: The Spin-Lock

We now have a crystal structure which should enable an accurate calculation of the Fermi contact shifts. Now we need to transform this into an input file. CRYSTAL expects an input file conveniently named INPUT. This is the only file required for calculation within a directory; other important files include:

- fort.9: the converged wavefunction
- fort.79: the previous self-consistent field (SCF) cycle wavefunction (if a calculation converged, this is the same as fort.9; if it did not or if it failed for other reasons, this will contain the most recent wavefunction)
- fort.20: the "guess previous" wavefunction: used for initialising the next calculation
- fort.34: the converged structure from a geometry optimization run
- fort.33: the structure obtained in the most recent SCF cycle (identical to fort.34 if converged; if not, this contains the most recent structure)

The only other mandatory file needed in the calculation directory is the binary file which will run CRYSTAL. This will look something like Figure 3.

The INPUT file may be broken up into three separate sections: (i) the geometry input block, (ii) the basis sets, and (iii) the DFT and spin input block.

3.2.1 The Geometry Block

This section is highlighted in Figure 4.

1. The title - you can provide any name you so choose in here *e.g.*, Li2MnO3

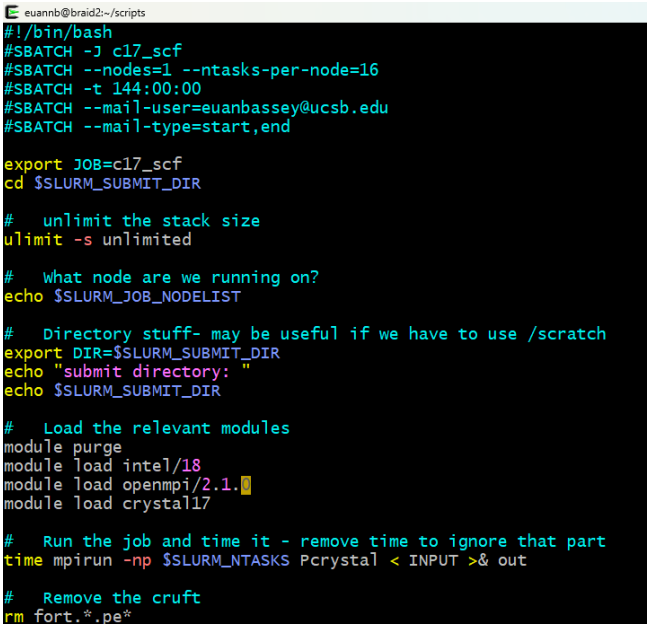

Figure 3: An example CRYSTAL17 bash job submission script. Note that this runs on slurm, but can also be used on PBS if commands are adjusted accordingly. The "mpirun" line is the part that actually runs CRYSTAL; you may require modules other than those listed here.

2. The type of calculation to be performed - here, we are dealing with a periodic crystalline system, so we call CRYSTAL (other options such as MOLECULE or POLYMER also exist). If we had a pre-converged structure, we could put "EXTERNAL" here and skip all remaining geometry lines, only needing the "ENDG" line; we must ensure that fort.34 is in the directory if EXTERNAL is specified) *e.g.*, CRYSTAL

3. The shift of origin coordinates, if desired: express as fractions of the crystallographic lattice vectors, multiplied by 24 to get integer values of the shifts; these values must be separated by a space *e.g.*, 0 0 0

4. The space group number of the structure. It is strongly recommended to switch symmetry off to better capture local distortions not observed from the average crystal structure. *e.g.*, 1

5. The lattice parameters, separated by spaces - all values relevant to the space group must be listed here, in the order a, b, c, α, β, γ *e.g.*, 9.903... 8.519... 9.588... 90 99.6... 90

6. The number of ions in the cell *e.g.*, 96

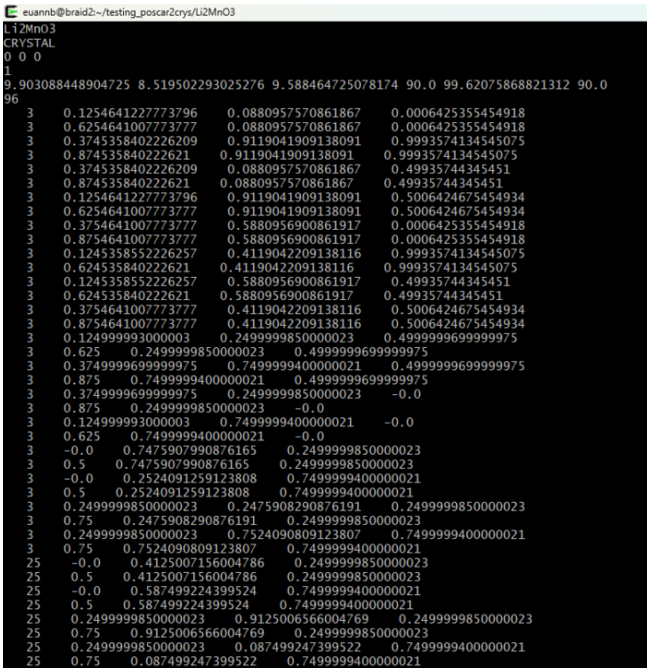

Figure 4: An example geometry section from a CRYSTAL17 INPUT file.

7. Lines 7 to ...: the atom identities and coordinates, separated by spaces. The first number is always an integer and corresponds to an atom and its specific basis. The second, third and fourth numbers are the x, y and z coordinates of the specific atom. If you want to specify the location of a specific oxidation state–perhaps you have four Mn^{3+} and twelve Mn^{4+}–you should label the numbers differently. Adding a 1 to the start of a number (*e.g.*, 25 becomes 125; 28 becomes 128) to distinguish the same chemical species but different oxidation states. *e.g.*, 3 0.125... 0.088... 0.0006... Note that this example corresponds to a lithium (number 3), whilst further down, manganeses are enumerated (number 25).

8. The end: a line which defines the end of the geometry block *e.g.*, ENDG

3.2.2 The Basis Sets

Next, we have the basis sets. A *Basis Set* is a mathematical function chosen to represent part or all of a wavefunction in a system. In periodic crystalline systems, these bases must obey *Bloch's theorem* which states that the wavefunctions of a crystal must be commensurate with the periodicity of the

underlying lattice. CRYSTAL uses *Localised Gaussian* basis sets, analogous to the linear combination of atomic orbitals approach for describing delocalised (multi-centre) electrons. The single-electron wavefunction, $\Psi_{n,k}(\mathbf{r})$, for one of the electronic states of a system may be written as a linear combination of functions, $\phi_{m,k}(\mathbf{r})$, which obey Bloch's theorem:

$$\Psi_{n,k}(\mathbf{r}) = \sum_{m} c_{n,m,k}\phi_{m,k}(\mathbf{r}), \tag{7}$$

where $c_{n,m,k}$ are unknown coefficients which must be determined. The functions $\phi_{m,k}(\mathbf{r})$ may be written as:

$$\phi_{m,k}(\mathbf{r}) = \sum_{\mathbf{g}} \phi_m(\mathbf{r} - \mathbf{A}_m - \mathbf{g})\exp(\mathrm{i}\mathbf{k}\cdot\mathbf{g}), \tag{8}$$

where $\phi_m(\mathbf{r})$ are the localised orbital functions centred at the coordinates of the nucleus, $\mathbf{A}_\mathsf{m}$, and the sum extends over all lattice vectors $\mathbf{g}$. This sum over all $\mathbf{g}$ results in orbitals which are replicated periodically throughout space, making the single-electron wavefunction periodic, as required. These orbital functions can be expressed as a linear combination of normalised Gaussian-type functions, $G(\alpha,\ \mathbf{r} - \mathbf{A}_m - \mathbf{g})$, known as *primitives*, so that:

$$\phi_m(\mathbf{r} - \mathbf{A}_m - \mathbf{g}) = \sum_{j}^{n_G} d_j G\left(\alpha_j,\ \mathbf{r} - \mathbf{A}_m - \mathbf{g}\right), \tag{9}$$

where d_j is a coefficient known as the contraction coefficient, α_j is the Gaussian exponent and n_G are the number of Gaussian primitives in the orbital function. The contraction coefficient describes the height of the Gaussian in the orbital function, whilst α_j describes the diffuseness of the Gaussian: small values of α_j typically describe diffuse electrons in the valence region, whilst large values generally describe localised core-like states. The quality of a calculation (*i.e.*, the ability to produce an accurate description of the electronic structure) using localised Gaussian bases is sensitive to the number of contracted Gaussian-type orbitals (GTOs), $\phi_\mathsf{m}(\mathbf{r})$, and number of primitives, n_G, used to describe each orbital. Accurate descriptions of the electronic structure typically require many GTOs, but this comes at a high computational cost.

The CRYSTAL website has a large library of basis sets available (see `https://www.crystal.`

`unito.it/basis_sets.html`) - click on the element of interest; this will take you to a web page containing a series of bases. These are, in general, made with a specific group of systems in mind, so it is recommended to check the reference for further information. As a general rule of thumb, you should aim to keep the number of shells of as similar as possible across the different species. The greater the number of shells, the more accurate but the more expensive a calculation gets. This section of the INPUT file is shown in Figure 5.

1. The first line of a basis set is given by the atomic number/identifier and the number of electronic shells in the basis, separated by a space. *e.g.*, 3 7 means the set for Li, with seven shells in the basis

2. The basis is then arranged into sub-blocks;

   - The first line contains five numbers:
     - The type of basis to be used: 0 for a 'general' basis; 1 for a Pople standard STO-nG;[vi] 2 for a Pople standard 3(6)-21G.[vii]
     - The shell type: 0 = $(1 \times s)$ orbital; 1 = $(1 \times s) + (3 \times p)$; 2 = $(3 \times p)$; 3 = $(5 \times d)$; 4 = $(7 \times f)$
     - The number of primitives in the shell
     - The number of electrons in the shell: this should be changed to change to oxidation state.
     - The scaling factor for the basis
   - The second line onwards contains the amplitude (contraction coefficient, d_j) and the diffuseness (α_j), separated by a space or tab

3. At the end of the basis set section, write:

99 0

[CHARGED - if using]

[vi] These are Slater-Type Orbitals (STOs) comprised of n Gaussian primitives. Recall that a Slater orbital is just a linear combination of atomic spin-orbitals.

[vii] Pople bases of the form x-yzG are, again, Gaussian primitives which account for valence orbitals differently to core orbitals. Here, x is the number of primitive Gaussians comprising each core atomic orbital basis function; Y and Z denote that each valence orbital is composed of two basis functions: one with y primitive Gaussians, the other with z.

PRINT

END

It is critical to ensure the number of electrons is correct for the oxidation state - the most common error in CRYSTAL is having a charged unit cell. The basis sets from the CRYSTAL website are given as the neutral atom unless stated otherwise.

3.2.3 DFT and Spin Commands

In the DFT block [Figure 6], we write:

- Start with 'DFT' as first line
- SPIN indicates spin-polarised calculation (i.e. a paramagnetic system with net unpaired spin density)
- For Hybrid functionals

DFT SPIN BECKE CORRELAT LYP

- BECKE indicates a GGA functional
- CORRELAT indicates a correlation functional (for GGA, LYP is commonly used)
- Note that DFT-D3 correction (for modelling Van der Waals forces) can be added using B3LYP-D3 as the functional
- NONLOCAL is the next line; defines non-local weighting parameters: on the following line, the first number tells you the exchange weight of the non-local part of exchange; the second number gives the weight of the non-local correlation
- HYBRID indicates the amount of mixing of Hartree-Fock and DFT (*i.e.*, HYBRID 100 gives 100% Hartree-Fock; 0 is pure DFT)
- XLGRID is an extra-large grid over which calculations are performed
- END finishes this section

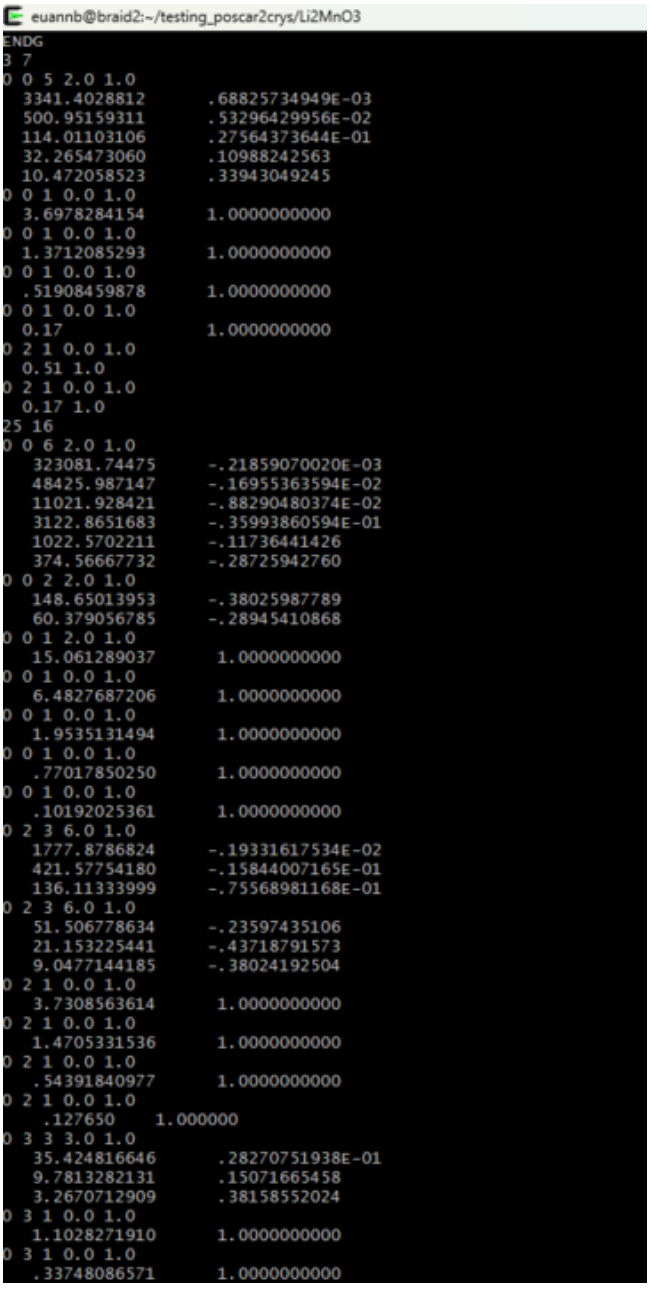

Figure 5: An example basis set section from a CRYSTAL17 INPUT file.

- TOLINTEG gives the tolerances of the different exchange and overlap integrals: a larger value (*e.g.*, 8 8 8 8 16) can be used when poorer basis sets are used, as these basis sets overlap less and therefore need a higher tolerance limit to produce a bonding interaction – *c.f.* smaller value 7 7 7 7 14; make sure that TOLINTEG remains the same between spin-lock and spin-relax calculations; also needs to be the same between spin-flip and spin-lock calculations

- SCFDIR: monoelectronic and bielectronic integrals are evaluated at each step; can switch off with NODIRECT

- SHRINK: the factor in reciprocal space to shrink the Pack-Monkhorst/Gilat net by; first number gives the shrinking factor in reciprocal space; second number gives a denser k-point net near the Fermi energy

- FMIXING: gives the percentage of Fock mixing – i.e. how much of the previous SCF wavefunction to use in the next cycle; if too large, can force stabilisation without being self-consistent. Good starting value: 70

- SPINLOCK: gives the details of spin-polarisation – first number is the number of up electrons minus the number of down electrons (for ferromagnetic state, this is just the number of unpaired electrons); second number is how many cycles to keep this spin polarisation going for

- ATOMSPIN defines how many (first number) and which atoms (list of indices) are spin-polarised; need to place a '+1' or '-1' next to the index to indicate spin polarity

- the amount of energy (in Hartrees) to separate the occupied orbital from the unoccupied (set to non-zero to avoid a material becoming a metal) – first number specifies the energy gap = (number)*0.1 Hartrees; second number tells you about 'locking state' – 0 = no locking; 1 = locks non-metallic state throughout the calculation

- (Direct Inversion of the Iterative Subspace convergence accelerator): activated by default, gives faster convergence, but can be uncontrolled – if NODIIS activated, DIIS is deactivated and FMIXING 30% + LEVSHIFT is implemented

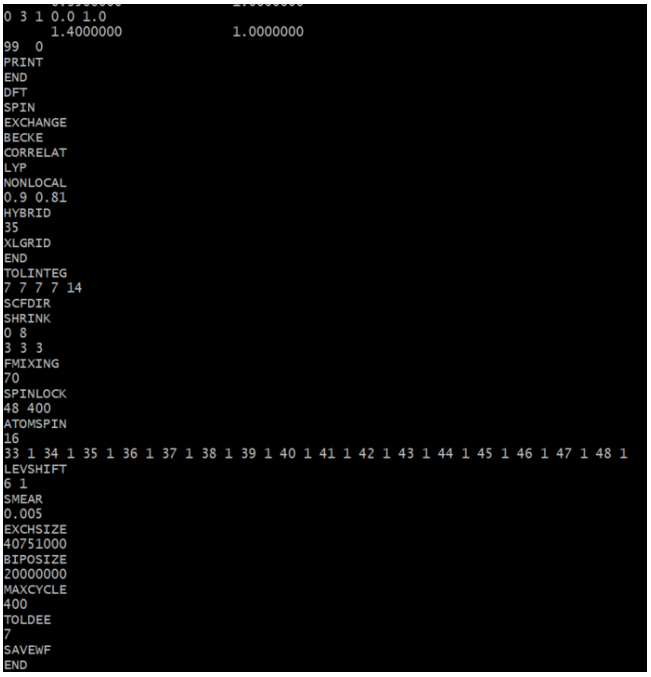

Figure 6: An example basis set section from a CRYSTAL17 INPUT file.

- temperature smearing of Fermi surface – modifies occupancy of eigenvalues according to the Fermi function (larger = more smearing: useful for metallic systems, where the sharp change in density of states causes unphysical oscillations in the charge density)
- EXCHSIZE: size of exchange bipolar expansion buffer (memory available on the node)
- BIPOSIZE: size of coulomb bipolar expansion buffer (memory available on the node)
- MAXCYCLE: number of SCF cycles to run
- TOLDEE: tolerance limit of change in energy between SCF cycles (number specifies limit as $10^{-\text{number}}$)
- SAVEWF: tells CRYSTAL to save the non-converged and converged wavefunctions as fort.79 and fort.9, respectively

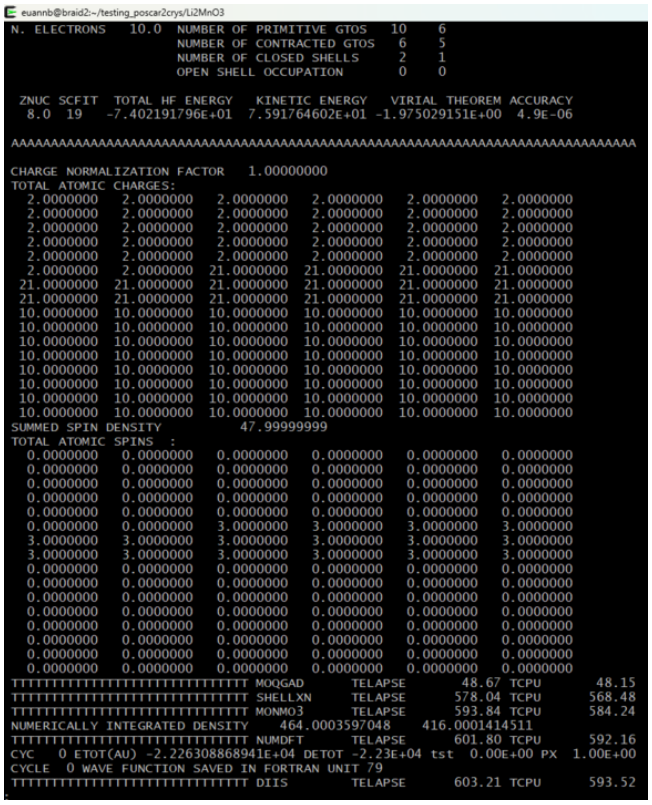

Figure 7: An example of the top section of an output file from a spin-locked calculation.

3.2.4 Running the calculation

The INPUT file is now complete, and CRYSTAL may be run. Note that we can run two levels of hybrid DFT: one with 35% Hartree-Fock and one with 20%; these provide upper and lower bounds, respectively, on the Fermi contact shift in most paramagnetic systems. The output file contains a long header describing the input information - crystal structure, DFT parameters and so on. After this, the SCF cycle results are presented: these appear as a table of charges and of spins. The initial values are exactly those which were input - for example 3 units of spin density (three unpaired electrons) for a Mn^{4+} [Figure 7].

Once converged, the spins of any diamagnetic centres is usually less than 0.2 units; paramagnetic centres have much larger values, but they do not always exactly equal the expected number of unpaired spins—*e.g.*, for three unpaired electrons, one might get 2.8 unpaired electrons. This is reflected in the converged spin densities [Figure 8].

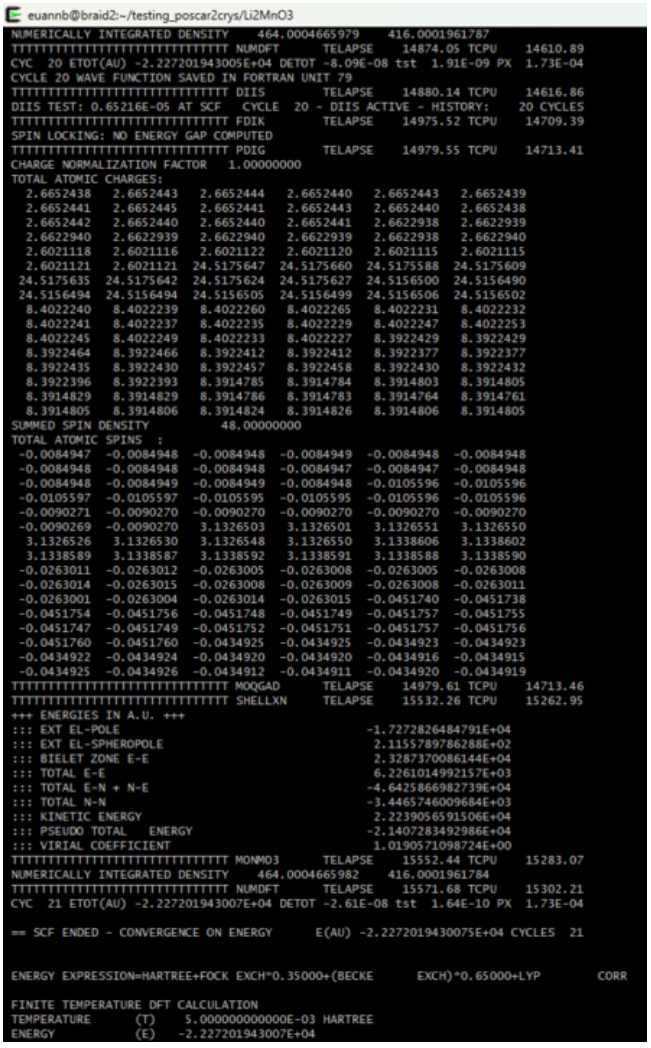

Figure 8: An example of the end section of an output file from a spin-locked calculation.

It is recommended to save useful files, specifically:

1. The "out" file (which can be copied to another output file for later use)
2. fort.9 - the converged wavefunction - move this to fort.20
3. The INPUT file (can also be copied to another file for later use/reference)

All other remaining files are not critical and can be deleted.

3.3 Step 2: The Spin-Relax

Having completed the spin-lock, we are now in a position to relax the wavefunction further without constraining the spins to be locked ferromagnetically. In almost all cases, the ferromagnetic state is retained; the purpose of this step is to minimise the electronic energy as much as possible.

The INPUT file can remain the same, save the following:

1. Remove all lines from SPINLOCK to SMEAR (and its proceeding SMEAR value) inclusive
2. Change FMIXING to 30 - to improve the stability of the calculation and avoid deviating too far from the ferromagnetic state
3. Add GUESSP on a new line, between SAVEWF and END, at the end of the INPUT file. Ensure that the "guessed" wavefunction (*i.e.*, the converged, spin-locked calculation wavefunction) is in the calculation directory as fort.20

The end of the INPUT file should now appear as in Figure 9.

The output from the spin relax has the same format as in the spin-locked calculation. In almost all cases, the wavefunction hardly changes and only a few SCF cycles are run; this can be checked in the spin and charge density table, as in Figure 10.

As in the spin-locked calculation, save the INPUT, out and fort.9 files for later use. All remaining files can be deleted.

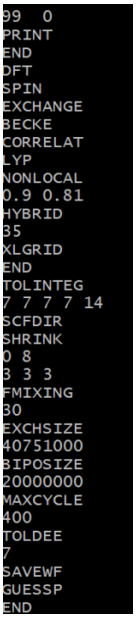

Figure 9: An example of the end section of an INPUT file from a spin-relaxed calculation.

3.3.1 Spin-Flipping

If bond pathways are desired, one can perform a spin-flip calculation. Use the converged wavefunction (fort.9) from either a converged spin-locked or spin-relaxed calculation as the guessed wavefunction (fort.20). Then, relative to a spin-locked INPUT file, change the following:

- Remove all lines from SPINLOCK to SMEAR (and its proceeding SMEAR value) inclusive
- Change FMIXING to 30 - to improve the stability of the calculation and avoid deviating too far from the ferromagnetic state
- After the FMIXING 30 lines, add:

SPINEDIT 1 Site number of desired flipped spin

- The first number after SPINEDIT corresponds to the number of spins to be flipped and the subsequent line is a space-separated list of the sites to be flipped (there is no need to specify the value to flip to, CRYSTAL will work this out - you only need give the site number)
- Add GUESSP on a new line, between SAVEWF and END, at the end of the INPUT file. Ensure

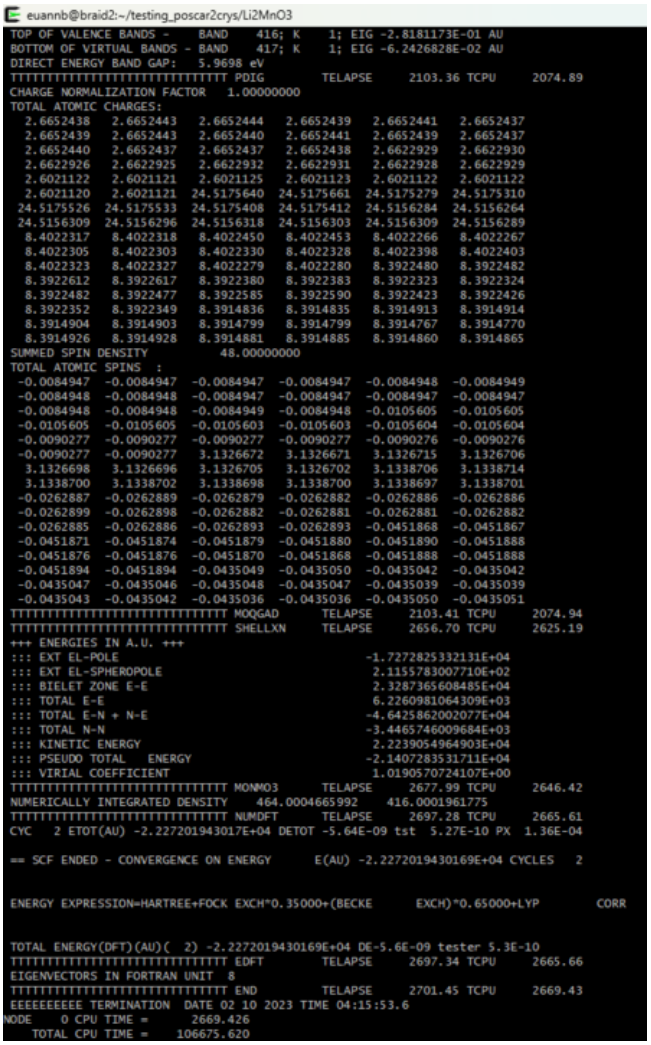

Figure 10: An example of the end of an output file from a spin-relaxed calculation.

that the "guessed" wavefunction (*i.e.*, the converged, spin-locked calculation wavefunction) is in the calculation directory as fort.20

3.4 Step 3: The Properties

With the calculation of the wavefunctions now complete, the spin densities at the nuclear positions may be extracted. Completely replace the contents of the INPUT file with that shown in Figure 11. The properties INPUT is as follows:

1. SETPRINT defines how much information should be printed: the first number requests the geometric information (atomic coordinates and lattice parameters); the second two extract the Fermi contact tensor

2. ANISOTRO computes the anisotropy tensor of the Fermi contact interaction tensor; ALL specifies to do this for all atoms in the cell

3. ISOTROPIC computes the isotropic hyperfine coupling and spin density at the nuclear positions, with ALL again requesting this for all atoms in the unit cell

4. POTC extracts the electrostatic potential (electric field gradient, EFG tensor, used for quadrupolar parameter calculations), its first and second derivative; the subsequent zeros requests the EFG to be computed at all positions in the cell

5. PPAN performs a Mulliken population analysis, including orbital, shell and atomic charges - this writes to a file called PPAN.DAT

6. NEWK computes the eigenvectors of the Hamiltonian for the system; the first two numbers after this tag are the shrinking factors for the primary and secondary reciprocal space net (the former is for diagonalising the Fock/Kohn-Sham matrix; the latter for evaluating the Fermi energy and density matrix) - this is needed for density of states calculations. The next three numbers give the reciprocal space vectors to sample for the density of states; the last two numbers calculate the Fermi energy and print it out.

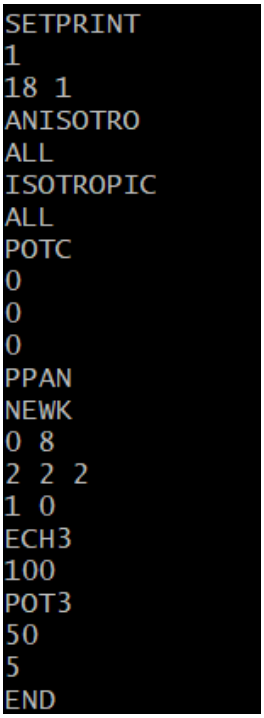

Figure 11: An example of the INPUT file for extracting properties from the wavefunction.

7. ECH3 computes the spin density map on a 3-d grid; the number afterwards dictates the number of points in the grid for each direction (x, y and z). This outputs to DENS_CUBE.DAT (for the charge density map) and SPIN_CUBE.DAT (for the spin density map) - both, if changed to .cube file formats, may be opened in a crystallography software package to visualise.

8. POT3 computes the electrostatic potential on a 3-d grid; the first number gives the number of points in the grid for each direction (x, y and z); the second number gives the penetration tolerance (recommended by the developers to be 5).

9. END ends the INPUT file

This may be run using the Pproperties CRYSTAL executable.[viii] The output files listed above are generated, alongside an 'out' file. Inside the 'out' file are the EFG and Fermi contact tensors; an example section of the spin density at nuclear positions, $|\psi^{\alpha-\beta}(\mathbf{R}_\mathrm{N})|^2$, is given in Figure 12.

[viii] This is not a typo: the executable is genuinely Pproperties.

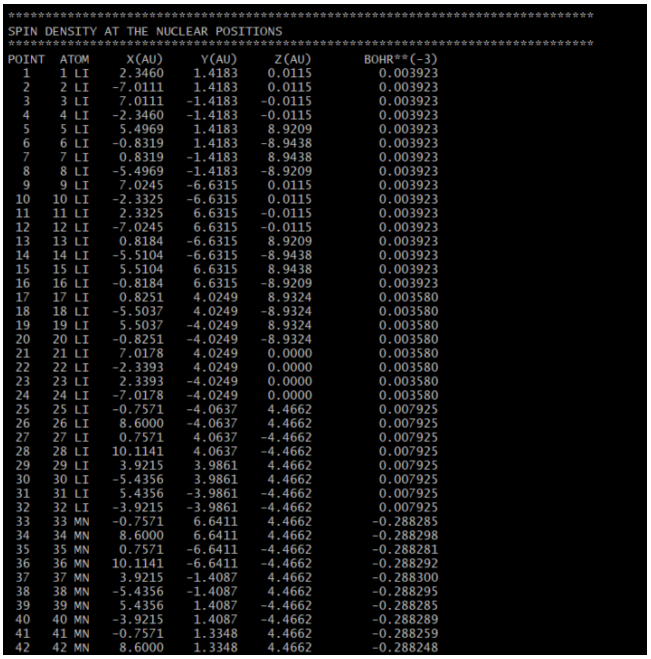

SPIN DENSITY AT THE NUCLEAR POSITIONS

POINT	ATOM	X(AU)	Y(AU)	Z(AU)	BOHR**(-3)
1	1 LI	2.3460	1.4183	0.0115	0.003923
2	2 LI	-7.0111	1.4183	0.0115	0.003923
3	3 LI	7.0111	-1.4183	-0.0115	0.003923
4	4 LI	-2.3460	-1.4183	-0.0115	0.003923
5	5 LI	5.4969	1.4183	8.9209	0.003923
6	6 LI	-0.8319	1.4183	-8.9438	0.003923
7	7 LI	0.8319	-1.4183	8.9438	0.003923
8	8 LI	-5.4969	-1.4183	-8.9209	0.003923
9	9 LI	7.0245	-6.6315	0.0115	0.003923
10	10 LI	-2.3325	-6.6315	0.0115	0.003923
11	11 LI	2.3325	6.6315	-0.0115	0.003923
12	12 LI	-7.0245	6.6315	-0.0115	0.003923
13	13 LI	0.8184	-6.6315	8.9209	0.003923
14	14 LI	-5.5104	-6.6315	-8.9438	0.003923
15	15 LI	5.5104	6.6315	8.9438	0.003923
16	16 LI	-0.8184	6.6315	-8.9209	0.003923
17	17 LI	0.8251	4.0249	8.9324	0.003580
18	18 LI	-5.5037	4.0249	-8.9324	0.003580
19	19 LI	5.5037	-4.0249	8.9324	0.003580
20	20 LI	-0.8251	-4.0249	-8.9324	0.003580
21	21 LI	7.0178	4.0249	0.0000	0.003580
22	22 LI	-2.3393	4.0249	0.0000	0.003580
23	23 LI	2.3393	-4.0249	0.0000	0.003580
24	24 LI	-7.0178	-4.0249	0.0000	0.003580
25	25 LI	-0.7571	-4.0637	4.4662	0.007925
26	26 LI	8.6000	-4.0637	4.4662	0.007925
27	27 LI	0.7571	4.0637	-4.4662	0.007925
28	28 LI	10.1141	4.0637	-4.4662	0.007925
29	29 LI	3.9215	3.9861	4.4662	0.007925
30	30 LI	-5.4356	3.9861	4.4662	0.007925
31	31 LI	5.4356	-3.9861	-4.4662	0.007925
32	32 LI	-3.9215	-3.9861	-4.4662	0.007925
33	33 MN	-0.7571	6.6411	4.4662	-0.288285
34	34 MN	8.6000	6.6411	4.4662	-0.288298
35	35 MN	0.7571	-6.6411	-4.4662	-0.288281
36	36 MN	10.1141	-6.6411	-4.4662	-0.288292
37	37 MN	3.9215	-1.4087	4.4662	-0.288300
38	38 MN	-5.4356	-1.4087	4.4662	-0.288295
39	39 MN	5.4356	1.4087	-4.4662	-0.288285
40	40 MN	-3.9215	1.4087	-4.4662	-0.288289
41	41 MN	-0.7571	1.3348	4.4662	-0.288259
42	42 MN	8.6000	1.3348	4.4662	-0.288248

Figure 12: An example of part of the spin density table inside the output properties file.

4 Appendix

4.1 Spin Dipolar Hyperfine

The spin dipolar hyperfine interaction tensor has components which are given by:

$$A_{ij}^{\mathrm{SD}} = \frac{\mu_0 \mu_{\mathrm{B}} \mu_{\mathrm{N}} g_{\mathrm{e}} \hbar \gamma_I}{8\pi S} \int \frac{3 r_i r_j - \delta_{ij} r^2}{r^5} |\psi^{\alpha-\beta}(\mathbf{r})|^2 \mathrm{d}^3 r, \tag{10}$$

where γ_I is the nuclear gyromagnetic ratio, r_i are the components of the vector between the unpaired electron and nuclear spin, r is the distance between them, and δ_{ij} the Kroenecker delta. These hyperfine couplings may be converted into shifts analogously to the isotropic shift, using eq. 4. The components of the spin-dipolar tensor are given by CRYSTAL and as such the full hyperfine tensor can be extracted and the spectrum predicted.

4.2 The Quadrupolar Interaction

Quadrupolar nuclei (whose nuclear spin is $I > \frac{1}{2}$) possess a nuclear electric quadrupole moment, Q, due to the non-spherical charge distribution in the nucleus. This moment interacts with the local electric field gradient (EFG) at the nucleus, which exists due to the local electronic and nuclear charge distribution. The quadrupolar interaction is described by a second-rank tensor, $\mathbf{V}$, giving the quadrupolar Hamiltonian:

$$\hat{H}_{\mathrm{Q}} = \frac{eQ}{2I(2I-1)\hbar}\hat{\mathbf{I}} \cdot \mathbf{V} \cdot \hat{\mathbf{I}} \tag{11}$$

where e is the elementary charge and eQ is the nuclear quadrupole moment; I is the nuclear spin; $\hbar$ the reduced Planck's constant and $\hat{I}$ the nuclear spin operator. The EFG tensor which may in turn be described by two terms—the anisotropy, eq, and the asymmetry, η_{Q}:

$$eq = V_{11} \tag{12}$$

$$\eta_{\mathrm{Q}} = \frac{V_{22} - V_{33}}{V_{11}}, \tag{13}$$

where V_{ii} are the principal components of the EFG tensor and $|\mathsf{V}_{11}| \geq |\mathsf{V}_{22}| \geq |\mathsf{V}_{33}|$. The asymmetry, η_{Q}, describes the degree of axial symmetry of the local coordination environment. The degree of spherical symmetry and the overall strength of the quadrupolar interaction is given by the quadrupolar coupling constant, C_{Q}:

$$C_{\mathrm{Q}} = \frac{e^2qQ}{\hbar}. \tag{14}$$

Sites with cubic or higher symmetry have $C_{\mathrm{Q}} = 0$, whilst less symmetric environments have non-zero C_{Q}.

If the quadrupolar coupling constant is much smaller than the applied magnetic field strength (typically the case for high-field NMR experiments), then the quadrupolar interaction may be considered as a perturbation of the nuclear Zeeman interaction. This shifts the Zeeman-split states so that they are no longer evenly spaced, generating several single-quantum ($\Delta m_I = \pm 1$) transitions. For half-integer nuclear spin quantum numbers I—such as ^{23}Na ($I = \frac{3}{2}$), ^{25}Mg ($I = \frac{5}{2}$) and ^{17}O ($I = \frac{5}{2}$)—these transitions can be split into two classes: the central transition (CT), corresponding

to $m_I = -\frac{1}{2} \longleftrightarrow +\frac{1}{2}$; and the satellite transition (ST), corresponding to all other single-quantum transitions [Figure 13]. To first order, the CT frequency is unaffected by quadrupolar coupling, but the (2*I*–1) ST frequencies have a second-rank orientational dependence, which can be averaged under MAS to generate a spinning sideband manifold.

For stronger quadrupolar interactions, both first- and second-order perturbations to the nuclear spin states must be considered [Figure 13]. Here, both the CTs and STs are orientation-dependent, but the anisotropy of these interactions cannot be averaged by MAS. In addition, the CT frequency changes, due to a change in the energy of the quadrupole-split states; this results in a quadrupole-induced shift: δ_{QIS}:

$$\delta_{\mathrm{QIS}} = -\frac{\nu_{\mathrm{Q}}^2}{30\nu_0^2}\left(I\left(I+1\right)-\frac{3}{4}\right)\left(1+\frac{\eta_{\mathrm{Q}}^2}{3}\right), \tag{15}$$

where ν_0 is the nuclear Larmor frequency (in Hz) and ν_{Q} the quadrupolar frequency (in Hz), defined as:

$$\nu_{\mathrm{Q}} = \frac{3C_{\mathrm{Q}}}{2I(2I-1)} \tag{16}$$

Since δ_{QIS} is proportional to $\frac{C_{\mathrm{Q}}^2}{\nu_0^2}$, this second-order term may be suppressed by using larger magnetic field strengths (*i.e.*, δ_{QIS} can be made negligible at high fields); higher fields also enable suppression of the additional broadening caused by the quadrupolar interaction. For systems with both hyperfine and quadrupolar interactions present, a compromise must be struck with the experimental field strength used.

CRYSTAL generates the EFG tensor, **V**, from which the quadrupolar shift may be extracted.

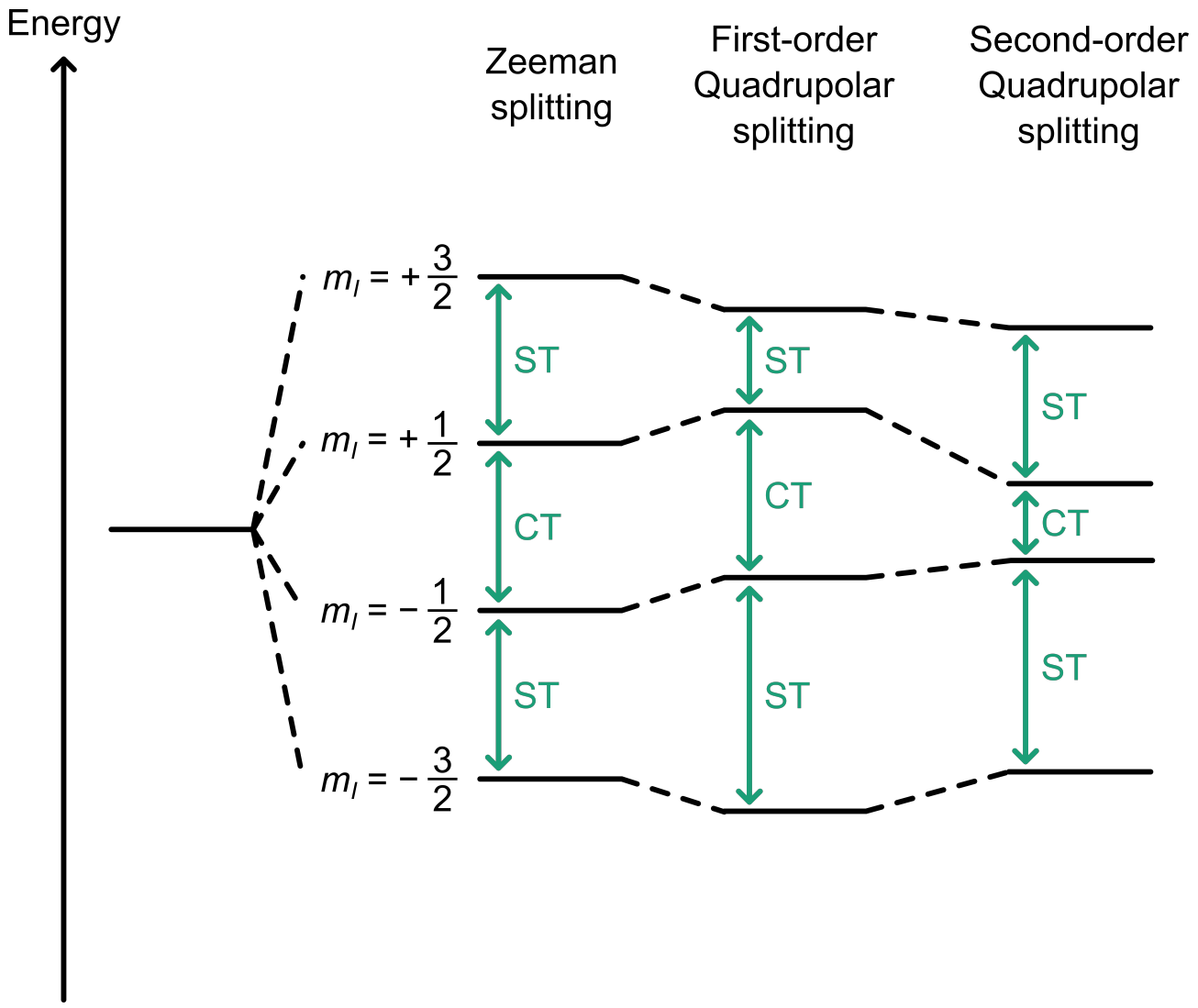

Figure 13: Schematic energy level diagram for a quadrupolar nucleus with $I = \frac{3}{2}$ (*e.g.*, ^{23}Na). The first splitting, due to the Zeeman interaction, occurs in the presence of an applied magnetic field. The quadrupolar splitting perturbs the Zeeman-split states to both first and second order. The central transition (CT) is only affected by the second-order perturbation, whilst satellite transition (ST) frequencies are affected by both first- and second-order perturbations.